



HAL
open science

Using Nitroxides To Model the Ion Mobility Behavior of Nitroxide-Ended Oligomers: A Bottom-up Approach To Predict Mobility Separation

Isaure Sergent, Thibault Schutz, Laurence Oswald, Georgette Obeid,
Jean-François Lutz, Laurence Charles

► To cite this version:

Isaure Sergent, Thibault Schutz, Laurence Oswald, Georgette Obeid, Jean-François Lutz, et al.. Using Nitroxides To Model the Ion Mobility Behavior of Nitroxide-Ended Oligomers: A Bottom-up Approach To Predict Mobility Separation. *Journal of The American Society for Mass Spectrometry*, 2024, 35 (3), pp.534-541. 10.1021/jasms.3c00393 . hal-04798578

HAL Id: hal-04798578

<https://hal.science/hal-04798578v1>

Submitted on 24 Nov 2024

HAL is a multi-disciplinary open access archive for the deposit and dissemination of scientific research documents, whether they are published or not. The documents may come from teaching and research institutions in France or abroad, or from public or private research centers.

L'archive ouverte pluridisciplinaire **HAL**, est destinée au dépôt et à la diffusion de documents scientifiques de niveau recherche, publiés ou non, émanant des établissements d'enseignement et de recherche français ou étrangers, des laboratoires publics ou privés.

Using nitroxides to model the ion mobility behavior of nitroxide-ended oligomers: a bottom-up approach to predict mobility separation

Isaure Sergent,¹ Thibault Schutz,^{2,3} Laurence Oswald,³ Georgette Obeid,² Jean-François Lutz,^{2,3*} and Laurence Charles^{1*}

¹ Aix Marseille Université, CNRS, UMR 7273, Institut de Chimie Radicalaire (ICR), 13397 Marseille Cedex 20, France

E-mail: laurence.charles@univ-amu.fr

² Université de Strasbourg, CNRS, Institut de Science et d'Ingénierie Supramoléculaires (ISIS), 67000 Strasbourg, France

E-mail: jflutz@unistra.fr

³ Université de Strasbourg, CNRS, Institut Charles Sadron UPR22, 67034 Strasbourg Cedex 2, France

Published in *Journal of the American Society for Mass Spectrometry*, 35, 524-541 (2024)

<https://pubs.acs.org/doi/abs/10.1021/jasms.3c00393>

Abstract.

Block-truncated poly(phosphodiester)s are digital macromolecules storing binary information that can be decoded by MS/MS sequencing of individual blocks released as primary fragments of the entire polymer. As such, they are ideal species for the serial sequencing methodology enabled by MS-(CID)-IMS-(CID)-MS coupling, where two activation stages are combined in-line with ion mobility spectrometry (IMS) separation. Yet, implementation of this coupling still requires efforts to achieve IMS resolution of inner blocks, that can be considered as small oligomers with α termination comprised of one nitroxide decorated with a different tag. As shown by molecular dynamics simulation, these oligomers adopt a conformation where the tag points out of the coil formed by the chain. Accordingly, the sole nitroxide termination was investigated here as a model to reduce the cost of calculation aimed at predicting the shift of collision cross section (CCS) induced by new tag candidates and extrapolate this effect to nitroxide-terminated oligomers. A library of 10 nitroxides and 7 oligomers was used to validate our calculation methods by comparison with experimental IMS data as well as our working assumption. Based on conformation predicted by theoretical calculation, three new tag candidates could be proposed to achieve the +40 \AA^2 CCS shift required to ensure IMS separation of oligomers regardless of their coded sequence.

INTRODUCTION

As inspired by DNA which stores large quantities of genetic information using a set of four monomers (A, T, G and C), digital polymers are sequence-defined macromolecules specifically designed for data storage applications.¹⁻³ These polymers are synthesized by stepwise solid-phase chemistry, making use of two comonomers arbitrarily defined as bits (*e.g.* the 0- and 1-bit of ASCII alphabet) to grow monodisperse and sequence-defined chains.⁴⁻⁶ Reading the binary information encoded in digital polymers is typically a sequencing task which can be achieved by tandem mass spectrometry (MS/MS),⁷ as now well established for peptides,⁸ oligonucleotides,⁹ and oligosaccharides.¹⁰ Yet, in contrast to biopolymers which structure is defined by nature to achieve biological functions, the main purpose of digital polymers is to be read: their structure can thus be specifically tailored to avoid usual roadblocks of MS/MS sequencing and hence derive maximum benefit of the technique. This is of utmost importance because full sequence coverage is mandatory for reliable reading of information in digital polymers. Indeed, unlike peptides which can be identified even from a partial sequence of amino acids after searching appropriate databases,¹¹ the set of 8 bits used to code a given letter in the selected ASCII alphabet may only differ by location of one 1-bit compared to the following letter, as exemplified with **01101001** coding for "i" *versus* **01101010** coding for "j".

Most commonly performed using collision-induced dissociation (CID), *de novo* MS/MS sequencing requires the random cleavage of the polymer backbone in order to produce complete sets of fragments that contain one or the other termination of the original chain and differ in mass by a single building unit. On the one hand, co-monomers of different mass must be selected so as to avoid the need for sophisticated approaches as implemented for peptides to distinguish isomeric residues such as leucine and isoleucine.^{12, 13} On the other hand, chemical moieties used to define the coding alphabet should not exhibit any reactivity upon activation so that backbone bond cleavages can occur independently of the co-monomer sequence. This is the reason why variation between coding units most often relies on alkyl groups, either with a simple H/CH₃ variation between the two units to implement a binary language,¹⁴⁻¹⁹ or employing a larger variety of alkyl segments to elaborate more complex alphabets.²⁰⁻²² Owing to the great variety of co-monomeric units that can be combined in their sequence, non-natural polymers do not obey universal fragmentation rules as do biopolymer families. This raises the particular issue of the reading direction which has to be defined as a convention between the "writer" and the "reader". For example, using the negative ion mode to sequence oligourethane chains deprotonated at their α chain-end ensures that all detected fragments contain this starting group: as a result, they need to be considered from the smallest to the largest in order to

reconstruct the sequence from the left- to the right-hand side.¹⁶ Placing isotopically-rich atoms such as bromine at the ω termination has also been a useful strategy to readily identify ω -containing fragments amongst other series in MS/MS spectra.^{14, 23} Ideally, the number of fragment series needs to be limited in order to prevent extensive signal dilution that would hamper full sequence coverage of chains as their size increases. In CID, energy imparted to precursor ions is indeed rapidly randomized, so any bonds of the structure may experience dissociation regardless of its location. This limits the size of sequenceable peptides to a few tens of residues and the same issue is encountered for abiological polymers.²⁴ Yet, since fragmentation of polymer ions in the gas phase is essentially dictated by their backbone chemistry,²⁵ the structure of digital polymers can also be optimized to tune their dissociation behavior. Beside lowering the number of reactive functions,²⁶ the most efficient strategy to minimize the variety of dissociation routes consists of introducing linkages of low dissociation energy that make any other bonds MS/MS silent. This was achieved by Zhang and co-workers who made use of the marked decrease of C–S bond dissociation energy upon oxidation of thioether into sulfoxide moieties,²⁷ whereas our group achieved full control of coded chain fragmentation with weak alkoxyamine linkages.²⁴ The latter approach was successfully employed to decipher, using a routine mass spectrometer, large amounts of information stored in digital poly(phosphodiester)s (PPDE) despite cleavage of phosphate bonds in each unit generates eight fragment series.²⁸ By distributing weak C–ON bonds between each group of eight co-monomers (*i.e.*, one byte of information), short coded blocks are released by soft activation of the chains and, when further subjected to CID, the complexity of their dissociation pattern remains manageable given their small size. Continuous improvements in the design of these block-truncated PPDEs have been achieved during the last five years to adjust crucial parameters, including their MS/MS readability,²⁹ enabling automated decryption of high capacity PPDEs containing up to 440 bits of information.²¹

Although error-free readout was systematically achieved, the analytical workflow implemented for these digital polymers lacks efficiency since it relies on multiple successive experiments, namely MS, MS/MS and pseudo-MS³, as described in **Figure S1** with the most recent structural design developed to also address the issue of atom economy.³⁰ The structure of block-truncated PPDEs was designed interactively with the development of this reading methodology.²⁸ In particular, to prevent any mass coincidence in MS² and enable safe selection of individual blocks for sequencing in the MS³ stage, each block is mass shifted with a specific label (hence named mass-tag). In order to take advantage of the resolving capabilities offered by orthogonal acceleration time-of-flight (oa-TOF) mass analyzers to safely assign fragments,

the Q-TOF instrument used here for MS and MS² stages was also employed to perform pseudo-MS³ experiments. As depicted in **Figure 1a**, deprotonated polymers are activated in the instrument interface by raising the cone (or skimmer) voltage to perform in-source CID; so-released individual blocks are then mass selected in the Q1 quadrupole for further excitation in the collision cell and fragments are measured in the oa-TOF. Although successfully enabling *de novo* sequencing of blocks with full sequence coverage (**Figure S1c**), this reading methodology is quite time consuming since the number of sequencing events increases with the number of blocks in the digital chain. The whole readout process would be advantageously accelerated by performing serial sequencing, with on-line separation of blocks prior to their sequencing. This could typically be achieved by combining the two activation steps with ion mobility spectrometry (IMS) in a single MS-(CID)-IMS-(CID)-MS experiment as enabled by Synapt instruments. Taking advantage of this instrumental configuration, the intact entire chain could be mass selected as the primary precursor ion in Q1, activated in the ion trap placed in front of the traveling wave ion mobility (TWIM) cell so that individual blocks released as fragments can reach the post-IMS collision cell one after the other for individual sequencing (**Figure 1b**). Of course, this hold true as long as blocks are all IMS-resolved.

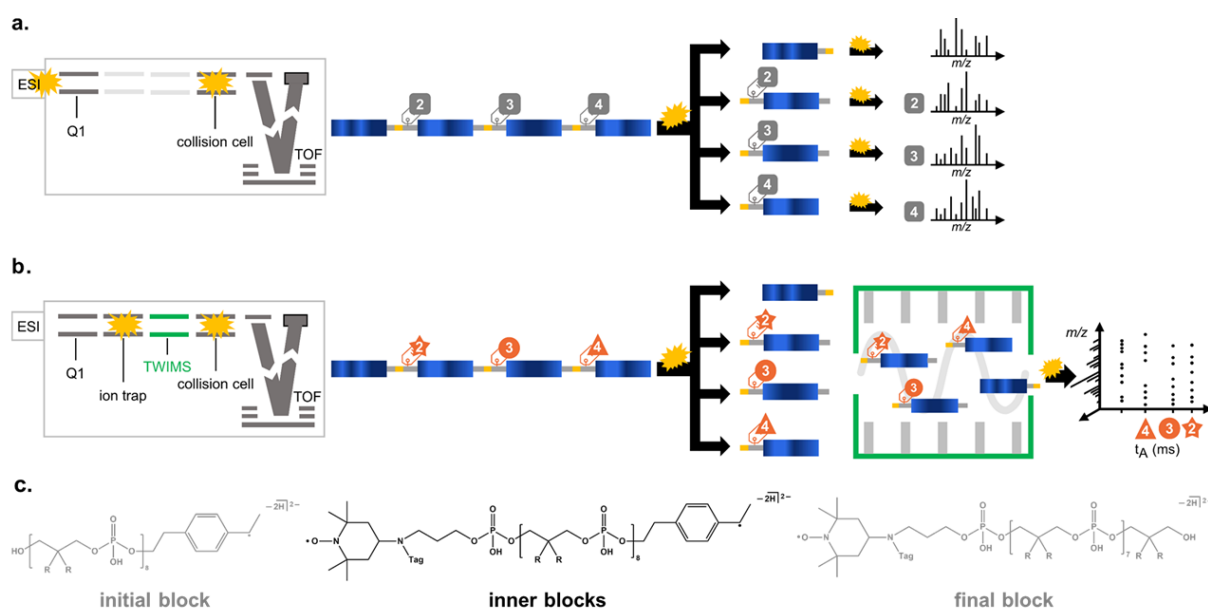


Figure 1. Instrumental configuration and analytical workflow a) used so far to implement the pseudo-MS³ steps requested to sequence all coded blocks and b) proposed to perform serial sequencing in a single MS-(CID)-IMS-(CID)-MS experiment. c) Detailed structure of individual blocks released upon C-ON bond cleavage as a function of their initial location in the PPDE chain (with R = H for 0-bit and R = CH₃ for 1-bit).

Preliminary IMS works indicated that blocks elute in the order of increasing mass (*i.e.* initial, final and inner block, **Figure 1c**), far earlier than larger fragments comprised of multiple blocks also released in the MS² step (**Figure S1b**). Moreover, when holding an appropriate tag, the final block could be IMS-separated from both the initial and inner blocks when all generated at the 2- charge state (data not shown). Although encouraging, these results indicate that efforts still need to be dedicated to IMS resolution of inner blocks, the number of which increases with the size of PPDE chains. Inner blocks share the same structure (**Figure 1c**) and can be regarded as small PDE oligomers holding a TEMPO-based radical decorated with one tag as the α group and the same carbon-centered radical ω group. Accordingly, the analytical question actually raised here is how the IMS behavior of these oligomers can be influenced by the nature of their α termination. In the present study, we have hence investigated the potential of the mass-tags, primarily conceived to enable mass-distinction of blocks, to also act as “shape-tags” able to induce IMS separation of inner blocks. Because it is dictated by ion collision cross section (CCS), IMS separation of these blocks was inferred from conformation predicted by theoretical calculation rather than performing the trial-and-error approach consisting of synthesizing polymers to experimentally evaluate the IMS impact of any tested tag.

EXPERIMENTAL SECTION

Chemicals. Water, methanol (MeOH) and acetonitrile (ACN) used to prepare solutions submitted to electrospray ionization (ESI) were from SDS (Peypin, France). Poly-DL-alanine (MW 1000–5000 Da), ammonium acetate and formic acid were purchased from Sigma Aldrich (St Louis, MO). Orthophosphoric acid (H₃PO₄, 85%) was from VWR International (Fontenay-sous-bois, France). All chemicals were used as received without further purification. TEMPO-based nitroxides as well as block-truncated PPDEs were prepared according to synthesis protocols detailed in a recent paper.³⁰ For ESI-IMS-MS analysis, PPDE samples (few mg) were dissolved in H₂O/ACN (50/50, v/v) supplemented with 0.1% formic acid, and further diluted (1/10, v/v) with MeOH whereas nitroxides (few mg) were dissolved in MeOH and further diluted (1/10, v/v) with a methanolic solution of ammonium acetate (3 mM).

Ion mobility mass spectrometry. High resolution mass spectrometry (MS) and traveling wave ion mobility (TWIM) spectrometry experiments were performed with a Synapt G2 HDMS instrument from Waters (Manchester, UK), operated in the negative ion mode for PPDEs (capillary ESI voltage, -2.27 kV; sampling cone voltage, -20 V; extraction cone voltage, -6 V) or in the positive ion mode for nitroxides (capillary ESI voltage, +2.8 kV; sampling cone voltage, +20 V; extraction cone voltage, +6 V). In both polarity modes, the desolvation gas (N₂)

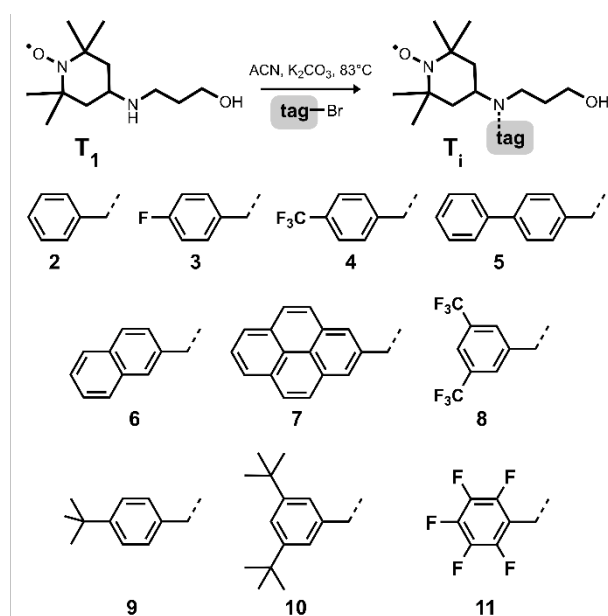
flow was 100 L/h at 35°C. In IMS-MS(/MS) experiments, ions were ejected from the ion trap into a cooling cell (helium flow: 180 mL/min) into the TWIM cell filled with N₂ (3.0 mbar) and operated in various wave height (WH, in V) and wave velocity (WV, in m/s) conditions. Ions were measured in the 150–1500 *m/z* range for PPDE blocks and 100–600 *m/z* range for nitroxides. A syringe pump was used to introduce sample solutions in the ESI source at a 10 μL/min flow rate. Instrument control, data acquisition and data processing of all experiments were achieved with the MassLynx 4.1 programs provided by Waters.

CCS calibration. Throughout the text, CCS values are designated according to the nomenclature proposed by Barran et al.³¹ Experimental arrival time distributions (ATDs) of ions were extracted manually from MassLynx software and arrival times (*t*_A) measured at peak apex were converted into experimental CCS (^{TW}CCS_{N₂→He}) using the IMSCal software.³² For nitroxides ionized in the positive ion mode, calibration standards were singly protonated poly-D,L-alanine oligomers³³ generated from a 0.1 mg/mL solution in H₂O/MeOH (10/90, v/v). For doubly deprotonated PPDE blocks in the negative mode, reference compounds were phosphoric acid clusters (1– and 2–)³⁴ formed upon ESI of a 2 mM solution in H₂O/ACN (50/50, v/v). As demonstrated in a recent study,³⁵ good quality CCS estimations can be obtained using the IMSCal model with no need for calibrants to match the chemical class of the analytes.

Molecular modeling and CCS calculation. For PPDE blocks, a multi-step protocol based on quantum methods (QM) and classical molecular dynamics (MD) was implemented. These molecules were constructed and protons manually removed from the phosphate groups, assuming an even distribution of the two charges (*i.e.* deprotonated sites located on phosphate groups 3 and 6).³⁶ Geometry optimization was performed at the semi-empirical level with AMPAC (Version 11 from SemichemInc., Shawnee, KS, USA) using the PM6 method.³⁷ Then, the RESP charges were calculated based on the Hartree-Fock method at the HF/6-31G(d) level with Gaussian16.³⁸ MD simulations of the doubly charged anions in vacuum were performed with GROMACS4.³⁹ These non-periodic simulations were run over 100 ns (time step 0.25 fs, 300 K, Berendsen thermostat) with no radial cut-offs for the non-bonded forces. Conformations were sampled every 1 ns from this trajectory. Protonated nitroxides were simulated using QM only. Geometry optimization was performed based on the Density Functional Theory (DFT) method at the B3LYP/6-31G(d) level, followed by RESP charges calculation based on the Hartree-Fock method at the uHF/6-31G(d) level, both with Gaussian16. In both cases, CCS values were calculated using the He-based trajectory method (TM) available in IMoS software⁴⁰ (default settings, 300 Pa). For PPDE blocks, ^{calc}CCS_{He} corresponds to the average value over the 100 sampled conformations.

RESULTS AND DISCUSSION

Conformation of inner blocks. Using a variety of block-truncated PPDEs prepared in a recent work,³⁰ experiments were first performed to assess the influence of available tags (**Scheme 1**) on the IMS behavior of inner blocks (further shortened to “blocks” for the sake of simplicity). On the one hand, when performing IMS-MS experiments for blocks containing different coded segments but the same tag, CCS is observed to slightly increase with the number of 1 units in their sequence: a systematic +5 Å² is measured upon substitution of monomer 0 (propyl phosphodiester) by monomer 1 (2,2-dimethylpropyl phosphodiester), regardless of their rank in the sequence (**Figure S2**). On the other hand, keeping the same coded segment but changing the tag also induces block CCS shift, the amplitude of which depends on the tag structure (**Figure S2**). However, regardless of the tag, the CCS of deprotonated blocks always spans a 40 Å² range as a function of the co-monomeric composition of their coded segment, from 0₈1₀ to 0₀1₈ (**Figure S2**). Overall, these findings strongly suggest that the tag and the composition of the coded segment both influence the whole block CCS but in an independent manner.



Scheme 1. Structure and designation of nitroxides T_2 - T_{11} used as reagents to introduce tags in block-truncated PPDEs.

In order to check whether this result can be explained by the geometry adopted by doubly deprotonated blocks in the gas phase, molecular dynamics simulation was performed. Only a

few cases were investigated due to the high time consumption (4 days) of each simulation. As illustrated in **Figure 2** for the biphenyl (**T₅**)- and naphthyl (**T₆**)-tagged blocks, these doubly charged species adopt the same type of conformation, with the tag pointing out of the coil formed by the coded segment. These geometries are supported by the fairly good agreement between CCS values calculated from 3D models and those experimentally determined by TWIMS analysis: $^{\text{calc}}\text{CCS}_{\text{He}} = 330 \text{ \AA}^2 (\pm 8 \text{ \AA}^2)$ vs $^{\text{TW}}\text{CCS}_{\text{N}_2 \rightarrow \text{He}} = 317 \text{ \AA}^2$ for the block labeled with **T₅**, $^{\text{calc}}\text{CCS}_{\text{He}} = 336 \text{ \AA}^2 (\pm 8 \text{ \AA}^2)$ vs $^{\text{TW}}\text{CCS}_{\text{N}_2 \rightarrow \text{He}} = 311 \text{ \AA}^2$ for the block labeled with **T₆**. Selection of sites 3 and 6 for deprotonation of two of the nine phosphate groups in these species might not correspond to the anionic forms actually measured by TWIMS, which could explain the slight overestimation obtained for calculated CCS values (+4% and +8%, respectively). It was hence very appealing to reduce the complexity of the system by considering the sole nitroxide termination of these PDE oligomers as a representative model to investigate the CCS impact of different tags.

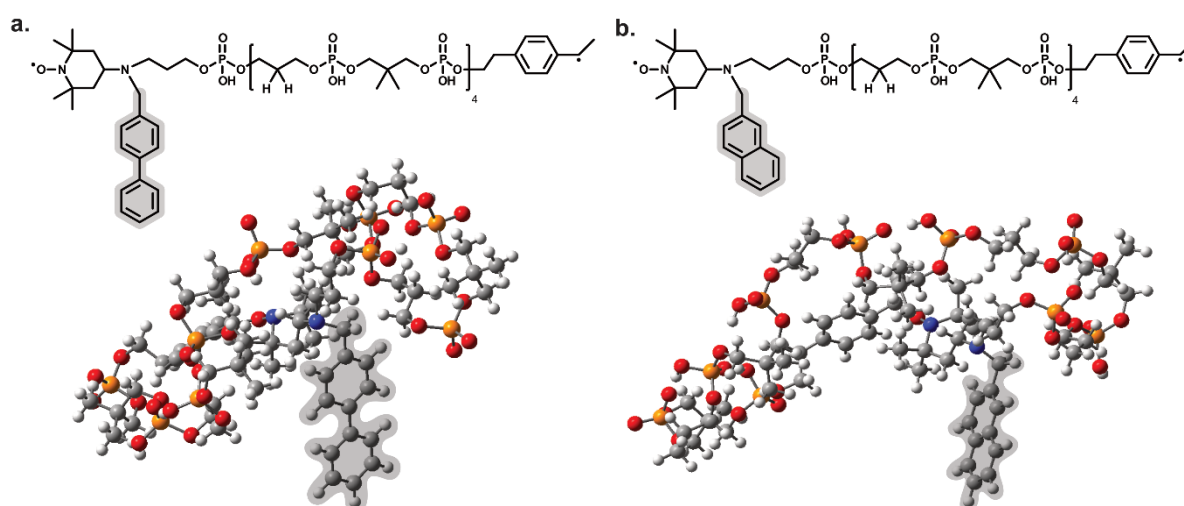


Figure 2. Geometry obtained by molecular dynamics simulation for blocks containing the same 01010101 coded segment and labeled with a) biphenyl (**T₅**) and b) naphthyl (**T₆**).

Validity of nitroxides to model nitroxide-ended oligomers. The validity of this assumption could be readily assessed since tagged nitroxides are available as reagents used in the preparation of PPDEs.³⁰ The ten nitroxides considered here (**Scheme 1**) were all prepared by reacting the secondary amine of the same 4-((3-hydroxypropyl)amino)-TEMPO (**T₁**) with different bromo-derivatives to afford the tagged nitroxides named **T₂**-**T₁₁**. These nitroxides, readily ionized as protonated species in positive mode ESI, were then analyzed by IMS-MS to first check whether they exhibit the same “elution” order compared to their block homologues.

As illustrated in **Figure 3**, arrival times of protonated nitroxides range from 3.25 ms for the smallest benzyl-tagged **T**₂ to 4.90 ms for the bulkiest di-*tert*butyl-benzyl-tagged **T**₁₀. Full width at half maximum (FWHM) of IMS peaks slightly increases with arrival time but remains consistent with the sole diffusion effects expected in the TWIMS cell (**Figure S3**). The same rough elution order was observed during IMS of the seven blocks available with the same **O**₄**14** coded segment (**Figure S4**), which is quite noteworthy owing to the fact that nitroxides and blocks were analyzed in different WH/WV TWIMS conditions (40/650 vs 40/450, respectively) and in different polarities, with **T**_{*i*} nitroxides as protonated species and **T**_{*i*}-tagged blocks as doubly deprotonated species.

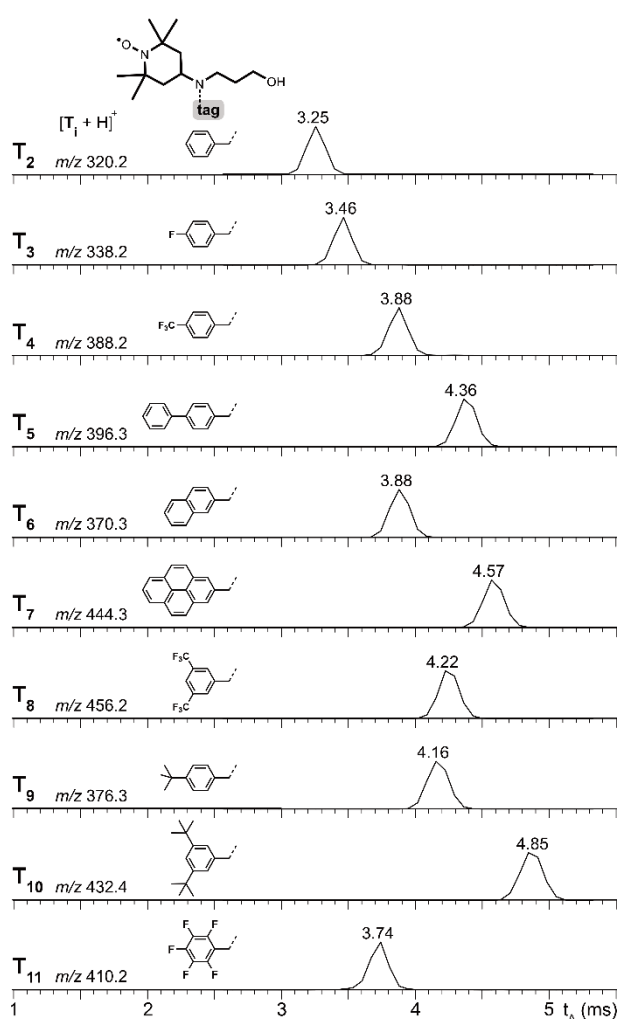


Figure 3. Arrival time (t_A) distribution of protonated nitroxides **T**₂-**T**₁₁, using WH = 40 V and WV = 650 m/s in the TWIM cell.

Even more interestingly in the context of this study, after arrival times have been converted into CCS values using appropriate calibration procedures (see experimental section), similar CCS

shifts are measured for nitroxides and blocks when switching from one tag to another. In other word, the ΔCCS difference between a given \mathbf{T}_i -tagged block and its \mathbf{T}_i nitroxide homologue remains roughly the same (**Table 1**). These experimental results validate the use of nitroxides as simplified models to perform simulation at lower calculation cost though providing relevant predictive information regarding the IMS behavior of nitroxide-ended oligomers.

	${}^{\text{TW}}\text{CCS}_{\text{N}_2 \rightarrow \text{He}} (\text{\AA}^2)$		$\Delta\text{CCS} (\text{\AA}^2)$
	$[\mathbf{T}_i\text{-block-2H}]^{2-}$	$[\mathbf{T}_i+\text{H}]^+$	
T₂	305	113	192
T₃	305	117	188
T₄	<i>n.a.</i>	127	-
T₅	317	138	179
T₆	311	127	184
T₇	320	142	178
T₈	311	134	177
T₉	314	133	181
T₁₀	<i>n.a.</i>	148	-
T₁₁	<i>n.a.</i>	123	-

Table 1. ${}^{\text{TW}}\text{CCS}_{\text{N}_2 \rightarrow \text{He}} (\text{\AA}^2)$ of \mathbf{T}_i -tagged blocks (comprising the same 01010101 coded segment) and of \mathbf{T}_i nitroxide homologues. *n.a.*: not available.

Molecular modeling was then performed for the 10 protonated \mathbf{T}_i nitroxides, considering two possible protomers in each case, with the proton located either on the nitroxide nitrogen ($\text{N}(\text{H}^+)\text{-O}$) or on the nitrogen atom connected to the tag ($\text{N}(\text{H}^+)\text{-tag}$). As documented in **Table S1**, energy calculation clearly shows that the $\text{N}(\text{H}^+)\text{-tag}$ protomer is always the most favored one (so the only one to be considered hereafter). Nevertheless, data in **Table S1** also show that ${}^{\text{calc}}\text{CCS}_{\text{He}}$ values are very similar for the two protomers. These calculated CCS are found to correlate quite nicely with experimental ${}^{\text{TW}}\text{CCS}_{\text{N}_2 \rightarrow \text{He}}$ values measured for protonated \mathbf{T}_i nitroxides (**Table 1**), as best emphasized in **Figure 4**, which supports the validity of the employed calculation methodology.

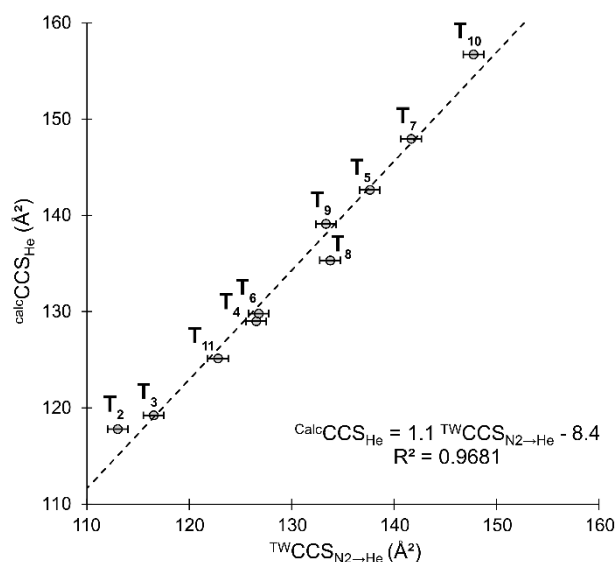


Figure 4. Correlation between calculated ($^{\text{calc}}\text{CCS}_{\text{He}}$) and experimental ($^{\text{TW}}\text{CCS}_{\text{N}_2 \rightarrow \text{He}}$) CCS of protonated T_i nitroxides. Error bars associated to $^{\text{TW}}\text{CCS}_{\text{N}_2 \rightarrow \text{He}}$ values reflects the $\pm 1 \text{ \AA}^2$ uncertainty provided by IMSCal.

Prediction of new tags. The calculation methodology being validated, it could then be used to safely predict CCS of nitroxides decorated with new tags, keeping in mind that candidates must fulfill the same “+40 \AA^2 CCS shift” requirement experimentally established for IMS separation of blocks in our instrument (*vide supra*). In order to rationalize the design of new tags, structure/property relationships were tentatively established for the 10 studied T_i nitroxides (**Figure 5**).

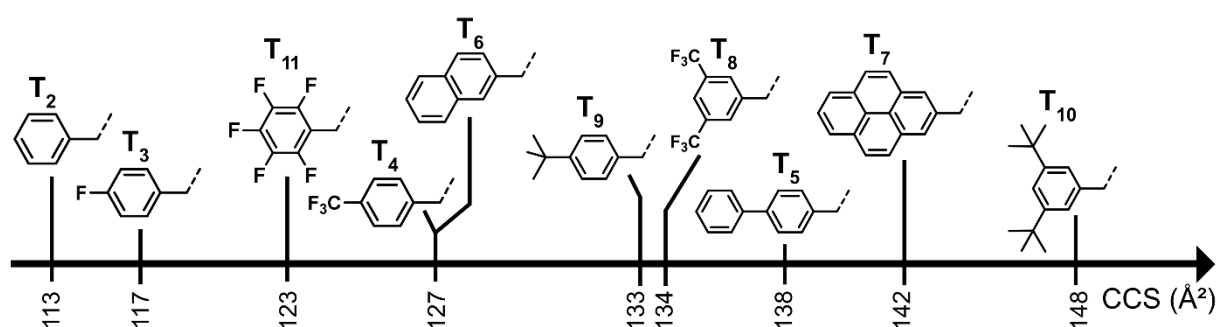


Figure 5. Ranking of $^{\text{TW}}\text{CCS}_{\text{N}_2 \rightarrow \text{He}}$ (\AA^2) measured for protonated T_i nitroxides as a function of their tag moiety.

Focusing on the effects of substituents on the aromatic ring as compared to the phenyl group in T_2 used hereafter as a reference:

- the modest effect of one fluorine atom in **T**₃ (+4 Å²) rapidly levels off, as shown with phenyl-F₅ in **T**₁₁ only exhibiting an overall +10 Å² CCS increase;
- the bulky *tert*-butyl group is more efficient at increasing CCS than CF₃ with +20 Å² for **T**₉ (*vs* +14 Å² for **T**₄) in singly substituted moieties and +35 Å² for **T**₁₀ (*vs* +21 Å² for **T**₈) in disubstituted moieties, respectively, but the CCS shift remains below the targeted +40 Å²;
- with CCS increase of +14 Å² for naphthyl in **T**₆ and +29 Å² for pyrenyl in **T**₇, condensation of aromatic rings seems to be a poorly efficient approach;
- in contrast, a string of aromatic rings appears as the most promising option, with a CCS increase of +25 Å² when switching from phenyl in **T**₂ to biphenyl in **T**₅.

Accordingly, strings with an increasing number of aromatic rings were considered for CCS calculation of nitroxides. As shown in **Figure 6**, the same +25 Å² increase is obtained upon each addition of one aromatic ring: as a result, the ter-, quater- and quique-phenyl tags all fulfill the +40 Å² requirement for safe IMS-resolution from the phenyl tagged-nitroxide (**T**₂).

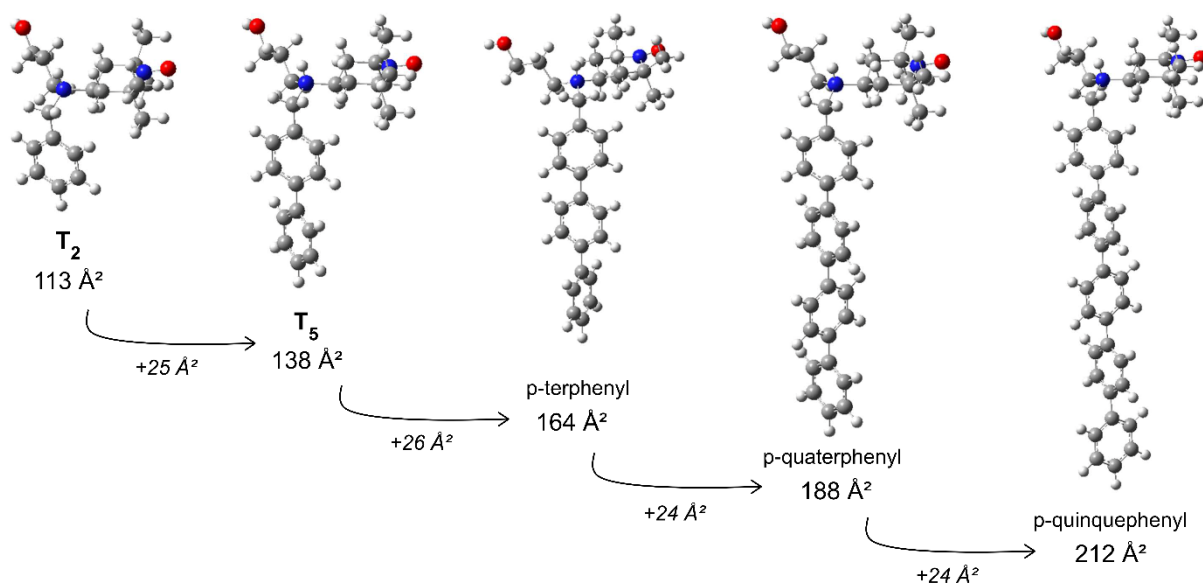


Figure 6. ^{calc}CCS_{He} (Å²) predicted for protonated nitroxide holding p-terphenyl, p-quaterphenyl and p-quinquephenyl tag, that is, an increasing number of phenyl rings compared to **T**₂ and **T**₅.

Extrapolating CCS differences calculated between these three candidates and **T**_{*i*} nitroxides (**Table S2**) to nitroxide-terminated PDE oligomers permits to envisage the MS-(CID)-IMS-(CID)-MS coupling to sequence tetrablock PPDEs, with the two inner blocks labelled with either p-quinquephenyl or p-quaterphenyl and any of the **T**_{*i*} tags. The p-terphenyl candidate can only be used in conjunction with **T**₂, **T**₃ or **T**₁₁, but adding the quinquephenyl tag would allow

IMS resolution of three inner blocks and hence serial sequencing of PPDEs comprised of five blocks.

CONCLUSIONS

This study is an additional demonstration that the structure of digital polymers can be adapted to best fit requirements of analytical methodologies conceived to improve their *de novo* sequencing. The design of tags enabling the IMS separation of inner blocks requested to perform serial sequencing in MS-(CID)-IMS-(CID)-MS was less straightforward than conception of mass-tag aimed at preventing their mass coincidence. Yet, capitalizing on the peculiar conformation of these blocks at the 2- charge state, with the tag pointing out of the coil formed by the coded segment, tagged nitroxides were shown to be relevant models for CCS predictions while minimizing calculation costs. It is worth mentioning that the 40 Å² CCS shift established here for safe separation of blocks is to be related to the quite low resolution of the instrument used in this study, and alternative IMS technologies offering higher resolving power should make this requirement less stringent. Of course, these predictions still remain to be validated experimentally but synthesis efforts can now be focused on preparation of PPDEs involving the sole tags predicted to induce IMS resolution of inner blocks. This is the reason why only para isomers have been considered when simulating CCS of nitroxides with an increasing number of aromatic rings: their bromo-derivatives are commercially available, which will facilitate the synthesis of the corresponding nitroxides to be involved in the preparation of block-truncated PPDEs. If successful, this will show that mass-tags can also be used as shape-tags to highly accelerate the readout protocol of these digital polymers.

ACKNOWLEDGMENTS

The authors thank the French National Research Agency for financial support (Project shapeNread, grant numbers ANR-19-CE29-0015-01 and ANR-19-CE29-0015-02). I.S. thanks the Doctorate School *Sciences Chimiques* of Aix Marseille University for her PhD fellowship. G.O. thanks the CSC Graduate School funded by the French National Research Agency (CSC-IGS ANR-17-EURE-0016) for a master fellowship. L.C. acknowledges support from Spectropole, the Analytical Facility of Aix-Marseille University, by granting a special access to the instruments purchased with European Funding (FEDER OBJ2142-3341). This work was also supported by the computing facilities of the *Centre Régional de Compétences en Modélisation Moléculaire* (CRCMM) of Aix Marseille University. For the polymer synthesis

part, this research work has been started at the Institut Charles Sadron (ICS) and finalized at the Institut de Science et d'Ingénierie Supramoléculaires (ISIS).

REFERENCES

- (1) Lutz, J.-F. Writing on Polymer Chains. *Acc. Chem. Res.* **2013**, *46* (11), 2696-2705.
- (2) Lutz, J.-F.; Ouchi, M.; Liu, D. R.; Sawamoto, M. Sequence-Controlled Polymers. *Science* **2013**, *341* (6146), 1238149.
- (3) Colquhoun, H.; Lutz, J.-F. Information-Containing Macromolecules. *Nat. Chem.* **2014**, *6* (6), 455-456.
- (4) Badi, N.; Lutz, J.-F. Sequence Control in Polymer Synthesis. *Chem. Soc. Rev.* **2009**, *38* (12), 3383-3390.
- (5) Solleder, S. C.; Schneider, R. V.; Wetzel, K. S.; Boukis, A. C.; Meier, M. A. R. Recent Progress in the Design of Monodisperse, Sequence-Defined Macromolecules. *Macromol. Rapid Commun.* **2017**, *38* (9), 1600711.
- (6) De Neve, J.; Haven, J. J.; Maes, L.; Junkers, T. Sequence-Definition from Controlled Polymerization: the Next Generation of Materials. *Polym. Chem.* **2018**, *9* (38), 4692-4705.
- (7) Charles, L. Tandem Mass Spectrometry Sequencing of Sequence-Controlled and Sequence-Defined Synthetic Polymers. In *Sequence-controlled polymers*, Lutz, J.-F. Ed.; Wiley-VCH Verlag GmbH & Co., 2018; pp 479-504.
- (8) Biemann, K. Laying the Groundwork for Proteomics - Mass Spectrometry from 1958 to 1988. *Int. J. Mass Spectrom.* **2007**, *259* (1-3), 1-7.
- (9) McLuckey, S. A.; Vanberkel, G. J.; Glish, G. L. Tandem Mass-Spectrometry of Small, Multiply Charged Oligonucleotides. *J. Am. Soc. Mass Spectrom.* **1992**, *3* (1), 60-70.
- (10) Domon, B.; Costello, C. E. A systematic Nomenclature for Carbohydrate Fragmentations in FAB-MS/MS Spectra of Glycoconjugates. *Glycoconj. J.* **1988**, *5* (4), 397-409.
- (11) Steen, H.; Mann, M. The ABC's (and XYZ's) of Peptide Sequencing. *Nat. Rev. Molec. Cell Biol.* **2004**, *5* (9), 699-711.
- (12) Wee, S.; O'Hair, R. A. J.; McFadyen, W. D. Side-Chain Radical Losses from Radical Cations Allows Distinction of Leucine and Isoleucine Residues in the Isomeric Peptides Gly-XXX-Arg. *Rapid Commun. Mass Spectrom.* **2002**, *16* (9), 884-890.
- (13) Zhokhov, S. S.; Kovalyov, S. V.; Samgina, T. Y.; Lebedev, A. T. An EThcD-Based Method for Discrimination of Leucine and Isoleucine Residues in Tryptic Peptides. *J. Am. Soc. Mass Spectrom.* **2017**, *28* (8), 1600-1611.

- (14) Roy, R. K.; Meszynska, A.; Laure, C.; Charles, L.; Verchin, C.; Lutz, J.-F. Design and Synthesis of Digitally Encoded Polymers that can be Decoded and Erased. *Nat. Commun.* **2015**, *6*, 7237.
- (15) Trinh, T. T.; Oswald, L.; Chan-Seng, D.; Charles, L.; Lutz, J.-F. Preparation of Information-Containing Macromolecules by Ligation of Dyad-Encoded Oligomers. *Chem. Eur. J.* **2015**, *21* (34), 11961-11965.
- (16) Gunay, U. S.; Petit, B. E.; Karamessini, D.; Al Ouahabi, A.; Amalian, J. A.; Chendo, C.; Bouquey, M.; Gigmes, D.; Charles, L.; Lutz, J.-F. Chemoselective Synthesis of Uniform Sequence-Coded Polyurethanes and Their Use as Molecular Tags. *Chem* **2016**, *1* (1), 114-126.
- (17) Cavallo, G.; Al Ouahabi, A.; Oswald, L.; Charles, L.; Lutz, J.-F. Orthogonal Synthesis of "Easy-to-Read" Information-Containing Polymers Using Phosphoramidite and Radical Coupling Steps. *J. Am. Chem. Soc.* **2016**, *138* (30), 9417-9420.
- (18) Mondal, T.; Greff, V.; Petit, B. E.; Charles, L.; Lutz, J.-F. Efficient Protocol for the Synthesis of "N-Coded" Oligo- and Poly(N-Substituted Urethanes). *ACS Macro Lett.* **2019**, *8* (8), 1002-1005.
- (19) Shi, Q. Q.; Yin, H.; Song, R. D.; Xu, J.; Tan, J. J.; Zhou, X.; Cen, J.; Deng, Z. Y.; Tong, H. M.; Cui, C. H.; et al. Digital Micelles of Encoded Polymeric Amphiphiles for Direct Sequence Reading and Ex Vivo Label-Free Quantification. *Nat. Chem.* **2023**, *15* (2), 257-270.
- (20) Boukis, A. C.; Meier, M. A. R. Data Storage in Sequence-Defined Macromolecules via Multicomponent Reactions. *Eur. Polym. J.* **2018**, *104*, 32-38.
- (21) Laurent, E.; Amalian, J.-A.; Schutz, T.; Launay, K.; Clément, J.-L.; Gigmes, D.; Burel, A.; Carapito, C.; Charles, L.; Delsuc, M.-A.; Lutz, J.-F. Storing the Portrait of Antoine de Lavoisier in a Single Macromolecule. *C. R. Chim.* **2021**, *24* (2), 69-76.
- (22) Roszak, I.; Oswald, L.; Al Ouahabi, A.; Bertin, A.; Laurent, E.; Felix, O.; Carvin-Sergent, I.; Charles, L.; Lutz, J.-F. Synthesis and Sequencing of Informational Poly(amino phosphodiester)s. *Polym. Chem.* **2021**, *12* (37), 5279-5282.
- (23) Soete, M.; De Bruycker, K.; Du Prez, F. Rewritable Macromolecular Data Storage with Automated Read-out. *Angew. Chem. Int. Ed.* **2022**, *61* (13), e202116718.
- (24) Amalian, J.-A.; Al Ouahabi, A.; Cavallo, G.; König, N. F.; Poyer, S.; Lutz, J.-F.; Charles, L. Controlling the Structure of Sequence-Defined Poly(phosphodiester)s for Optimal MS/MS Reading of Digital Information. *J. Mass Spectrom.* **2017**, *52* (11), 788-798.
- (25) Wesdemiotis, C.; Solak, N.; Polce, M. J.; Dabney, D. E.; Chaicharoen, K.; Katzenmeyer, B. C. Fragmentation Pathways of Polymer Ions. *Mass Spectrom. Rev.* **2011**, *30* (4), 523-559.

- (26) Charles, L.; Cavallo, G.; Monnier, V.; Oswald, L.; Szweda, R.; Lutz, J.-F. MS/MS-Assisted Design of Sequence-Controlled Synthetic Polymers for Improved Reading of Encoded Information. *J. Am. Soc. Mass Spectrom.* **2017**, *28* (6), 1149-1159.
- (27) Liu, B. L.; Shi, Q. N.; Hu, L. H.; Huang, Z. H.; Zhu, X. L.; Zhang, Z. B. Engineering Digital Polymer Based on Thiol-Maleimide Michael Coupling Toward Effective Writing and Reading. *Polym. Chem.* **2020**, *11* (10), 1702-1707.
- (28) Al Ouahabi, A.; Amalian, J.-A.; Charles, L.; Lutz, J.-F. Mass Spectrometry Sequencing of Long Digital Polymers Facilitated by Programmed Inter-Byte Fragmentation. *Nat. Commun.* **2017**, *8*, 967.
- (29) Charles, L.; Lutz, J.-F. Design of Abiological Digital Poly(phosphodiester)s. *Acc. Chem. Res.* **2021**, *54* (7), 1791-1800.
- (30) Schutz, T.; Sergent, I.; Obeid, G.; Oswald, L.; Al Ouahabi, A.; Baxter, P. N. W.; Clément, J.-L.; Gignes, D.; Charles, L.; Lutz, J.-F. Conception and Evaluation of a Library of Cleavable Mass Tags for Digital Polymers Sequencing. *Angew. Chem. Int Ed.* **2023**, *62* (45), e202310801.
- (31) Pacholarz, K. J.; Barran, P. E. Distinguishing Loss of Structure from Subunit Dissociation for Protein Complexes with Variable Temperature Ion Mobility Mass Spectrometry. *Anal. Chem.* **2015**, *87* (12), 6271-6279.
- (32) Richardson, K.; Langridge, D.; Dixit, S. M.; Ruotolo, B. T. An Improved Calibration Approach for Traveling Wave Ion Mobility Spectrometry: Robust, High-Precision Collision Cross Sections. *Anal. Chem.* **2021**, *93* (7), 3542-3550.
- (33) Allen, S. J.; Giles, K.; Gilbert, T.; Bush, M. F. Ion Mobility Mass Spectrometry of Peptide, Protein, and Protein Complex Ions using a Radio-Frequency Confining Drift Cell. *Analyst* **2016**, *141* (3), 884-891.
- (34) Calabrese, V.; Lavanant, H.; Rosu, F.; Gabelica, V.; Afonso, C. Collision Cross Sections of Phosphoric Acid Cluster Anions in Helium Measured by Drift Tube Ion Mobility Mass Spectrometry. *J. Am. Soc. Mass Spectrom.* **2020**, *31* (4), 969-981.
- (35) Sergent, I.; Adjieufack, A. I.; Gaudel-Siri, A.; Siri, D.; Charles, L. The IMSCal Approach to Determine Collision Cross Section of Multiply Charged Anions in Traveling Wave Ion Mobility Spectrometry. *Int. J. Mass Spectrom.* **2023**, *492*, 117112.
- (36) Hoaglund, C. S.; Liu, Y. S.; Ellington, A. D.; Pagel, M.; Clemmer, D. E. Gas-Phase DNA: Oligothymidine Ion Conformers. *J. Am. Chem. Soc.* **1997**, *119* (38), 9051-9052.
- (37) Stewart, J. J. P. Optimization of Parameters for Semiempirical Methods V: Modification of NDDO Approximations and Application to 70 Elements. *J. Molec. Model.* **2007**, *13* (12), 1173-1213.

- (38) Frisch, M. J.; Trucks, G. W.; Schlegel, H. B.; Scuseria, G. E.; Robb, M. A.; Cheeseman, J. R.; Scalmani, G.; Barone, V.; Petersson, G. A.; Nakatsuji, H.; Li, X.; Caricato, M.; Marenich, A. V.; Bloino, J.; Janesko, B. G.; Gomperts, R.; Mennucci, B.; Hratchian, H. P.; Ortiz, J. V.; Izmaylov, A. F.; Sonnenberg, J. L.; Williams-Young, D.; Ding, F.; Lipparini, F.; Egidi, F.; Goings, J.; Peng, B.; Petrone, A.; Henderson, T.; Ranasinghe, D.; Zakrzewski, V. G.; Gao, J.; Rega, N.; Zheng, G.; Liang, W.; Hada, M.; Ehara, M.; Toyota, K.; Fukuda, R.; Hasegawa, J.; Ishida, M.; Nakajima, T.; Honda, Y.; Kitao, O.; Nakai, H.; Vreven, T.; Throssell, K.; Montgomery Jr, J. A.; Peralta, J. E.; Ogliaro, F.; Bearpark, M. J.; Heyd, J. J.; Brithers, E. N.; Kudin, K. N.; Staroverov, V. N.; Keith, T. A.; Kobayashi, R.; Normand, J.; Raghavachari, K.; Rendell, A. P.; Burant, J. C.; Iyengar, S. S.; Tomasi, J.; Cossi, M.; Millam, J. M.; Klene, M.; Adamo, C.; Cammi, R.; Ochterski, J. W.; Martin, R. L.; Morokuma, K.; Farkas, O.; Foresman, J. B.; Fow, D. J. *Gaussian 16*, Gaussian Inc.: Wallingford, CT, 2016.
- (39) Hess, B.; Kutzner, C.; van der Spoel, D.; Lindahl, E. GROMACS 4: Algorithms for Highly Efficient, Load-Balanced, and Scalable Molecular Simulation. *J. Chem. Theory Comput.* **2008**, *4* (3), 435-447.
- (40) Larriba-Andaluz, C.; Hogan, C. J. Collision Cross Section Calculations for Polyatomic Ions Considering Rotating Diatomic/Linear Gas Molecules. *J. Chem. Phys.* **2014**, *141* (19), 194107.